lubricants

MDPI

Article

Wear Study of Cubic Boron Nitride (cBN) Cutting Tool for Machining of Compacted Graphite Iron (CGI) with Different Metalworking Fluids

Long Zhu [1], Robert Evans [2], Yan Zhou [2,*] and Fei Ren [1,*]

[1] Department of Mechanical Engineering, Temple University, Philadelphia, PA 19122, USA; long.zhu@temple.edu
[2] Quaker Houghton, Conshohocken, PA 19428, USA; bob.evans@quakerhoughton.com
* Correspondence: yan.zhou@quakerhoughton.com (Y.Z.); renfei@temple.edu (F.R.)

Abstract: Due to its desirable mechanical properties, compacted graphite iron (CGI) has been used to replace conventional gray cast iron (CI) in various applications, such as automotive engine blocks and cylinder heads. However, the poor machinability of CGI can lead to excessive tool wear and consequently high manufacturing costs. Various strategies have been developed to improve the machinability of CGI, including optimizing machining parameters and the development of novel metalworking fluids. In this study, machining of CGI was conducted using cubic boron nitride (cBN) tools under different cutting speeds, with both soluble and full-synthetic water-based metalworking fluids at different levels of sulfur addition and water dilution. The effects of the metalworking fluids on the tool wear behavior were examined. Results showed that at 200 m/min cutting speed, the soluble metalworking fluid at 4% dilution and 0.3% sulfur compound exhibited the best performance, with a cutting distance reaching 23.8 km. In contrast, the least effective soluble metalworking fluid at 9% dilution and 0.3% sulfur compound resulted in a 28.6% decrease in the cutting distance (17.0 km) compared to the best one. At a higher speed (300 m/min), the cutting distance for all metalworking fluids dropped to less than 6.0 km, with the full-synthetic metalworking fluid showing the shortest cutting distance of 4.8 km.

Keywords: compacted graphite iron (CGI); cubic boron nitride (cBN); machining; metalworking fluid; wear

check for updates

Citation: Zhu, L.; Evans, R.; Zhou, Y.; Ren, F. Wear Study of Cubic Boron Nitride (cBN) Cutting Tool for Machining of Compacted Graphite Iron (CGI) with Different Metalworking Fluids. *Lubricants* **2022**, *10*, 51. https://doi.org/10.3390/lubricants10040051

Received: 26 January 2022
Accepted: 23 March 2022
Published: 26 March 2022

1. Introduction

Compacted graphite iron (CGI) has attracted much attention in the past decades to replace conventional cast irons in many industrial applications. For example, automotive engine blocks are usually made from gray cast iron (CI). In comparison to CI, CGI exhibits at least 35% higher elastic modulus, 70% higher tensile strength, and 80% higher fatigue limits [1]. Therefore, CGI engines are expected to achieve higher power output and better fuel economy [2]. The different mechanical properties between CGI and CI are related to their microstructural and compositional differences. The graphite flakes in CI result in a high level of discontinuities and facilitate crack initiation and propagation, leading to weak and brittle mechanical properties. On the other hand, the entangled coral-like graphite structures in CGI can reduce the level of discontinuity and stress concentration, and thus eliminate natural cleavage path, contributing to high strength and toughness [3,4].

It is commonly observed that CI possesses better machinability. One of the factors involved is the formation of a protective MnS layer. This pliable and soft MnS layer has been found to provide a lubrication effect and act as a barrier on tools against oxidation and diffusion during machining of CI [3,5]. However, since compacted graphite particles are only stable at low sulfur and oxygen contents, CGI is produced with sulfur that is about 10% of that in CI. In addition to the low sulfur content, Mg was added to further scavenge any excess oxygen and sulfur during the production of CGI. Since Mg has a high affinity with sulfur, MgS was formed preferentially to MnS [3].

Cubic boron nitride (cBN) is known to be the second hardest material next to diamond, and the good thermal and chemical stability of cBN renders it as a substitute for diamond-based cutting tools [6]. When cBN was used in high speed (>400 m/min) continuous cutting operations of CGI, such as turning, the tool life was 10–20 times shorter than that obtained with CI [7]. Tasdelen et al. [8] found that cBN tools had shorter tool life for turning CGI in comparison to CI, which was attributed to the higher temperature and more severe degradation of the insert from longer chips and chip-insert contact time [8].

Sulfur-based additives in metalworking fluids showed good potential of protecting cutting tools by forming a protective layer, reducing the friction and tool wear. Alves et al. [9] investigated the CGI drilling process with cemented carbide twist drills with different cutting fluids with and without sulfur extreme pressure (EP) additives. The results showed that the tool life was increased by 67% with the sulfur EP additive in the cutting fluid, comparing to no EP addition. The friction and wear were reduced because of the formed protective layer that contained S, Ti, and Al. Furthermore, when reacted with the metal surface, the sulfur-based additives could also reduce the adhesion at the tool-metal interface, preventing the generation of an adhesion bridge [9]. Evans et al. [4] used sulfur-based additives to compensate for the low level of sulfur in CGI to improve the machining of CGI. The results showed that sulfur-based additives could promote the formation of a protective layer [4].

Therefore, developing high-performance metalworking fluids to extend tool life is of great interest in the machining of CGI. In this study, machining of CGI was conducted using cBN tools under different cutting speeds, with four water-based metalworking fluids (three soluble fluids and one full-synthetic fluid) at different levels of sulfur addition and water dilution. Various characterization techniques were utilized to study the wear of cBN tools. The morphology of the cutting tool was examined using scanning electron microscopy (SEM) and 3D laser scanning confocal microscopy, while the chemistry was studied through energy dispersive X-ray spectroscopy (EDX) and transmission electron microscopy (TEM).

2. Experimental Sections

2.1. Materials

The CGI workpieces (grade: CGI-450) used in this study were obtained from SinterCast. The detailed composition information is shown in Table 1, and the microstructural and mechanical data provided by the supplier are shown in Table 2. The ceramic-coated cBN cutting tools (grade: BNC500) were purchased from Sumitomo Electric Carbide, Inc. The thickness of the coating is about 4.5 μm, as determined by SEM measurement. The cutting tool has a thickness of 4.76 mm and a nose radius of 0.8 mm. Each tool piece has four 12 mm-long cutting edges.

Table 1. Elemental composition of the CGI workpiece.

Element	C	Si	Mn	S	Cr	Cu	Mg	Sn	Ti	Fe
Percentage (%)	3.53	2.19	0.39	0.007	0.029	0.93	0.011	0.079	0.007	92.827

Table 2. Microstructural and mechanical data of the CGI workpiece.

Nodularity	CGI	Pearlite	BHN (750/5)	Yield 0.2%	UTS	Elongation
10%	90%	>95%	274 MPa	410 MPa	546 MPa	1.6%

Note: The percentage nodularity is calculated according to the SinterCast CGI Microstructure Rating Chart. The Brinell hardness and the tensile data are obtained from a standard test bar (DIN 1693/SS-112,127).

Three soluble metalworking fluids (based on MWF-A) and one full-synthetic metalworking fluid (based on MWF-B) were prepared with additional sulfur compound and different levels of water dilution (Quaker Houghton, Conshohocken, PA, USA). Tap water was used for the dilution, with a water hardness of 200 ppm. The composition of the metal working fluids is shown in Table 3.

Table 3. Information on the metalworking fluids used in this study.

Fluid	Composition	Use Concentration (%)	Total Sulfur Compound in Fluid (wt.%)
1	MWF-A	9	0.27
2	MWF-B	9	0
3	MWF-A	9	0.81
4	MWF-A	4	0.3

2.2. Turning Experiments

Longitudinal turning operations of CGI cylinders were conducted with a feed rate of 0.3 mm/revolution and depth of cut of 0.2 mm at two different cutting speeds: 200 m/min, 300 m/min. The flank wear was measured by using an optical microscope with maximum flank wear reaching 0.25 mm as a failure. The inserts were retrieved at certain stages of the cutting process for flank wear measurement.

2.3. Characterization

The morphology of the flank face of the inserts was examined through scanning electron microscopy (SEM, Quanta450 FEG SEM, FEI Inc., Hillsboro, OR, USA). The elemental composition and distribution were investigated through energy dispersive X-ray spectroscopy (EDX). Electron diffraction using a transmission electron microscope (TEM, JEM-1400, JEOL, Tokyo, Japan) was further utilized to characterize the chemistry of the worn flank surface. For TEM investigation, the deposition on the worn flank surface was scraped using sharp tweezers. The collected powder was sonicated and dispersed in isopropanol. The dispersion was then pipetted onto a copper grid and examined through TEM. The roughness in the cBN grain region of the flank face of the tool was measured by a 3D laser scanning confocal microscope (Keyence VK-X1000, Keyence Corp., Osaka, Japan) with a scan size of $20 \times 20\ \mu m^2$.

3. Results and Discussions

The progressive flank wear on cutting inserts was measured by an optical microscope at different speeds (200 m/min and 300 m/min) with four metalworking fluids. The results are presented in Figure 1. At 200 m/min cutting speed, as shown in Figure 1a, fluid #4 (containing the most water; Table 2) exhibited the best performance, with the cutting distance reaching 23.8 km before failure. Fluid #1 showed the least effective performance, with the cutting distance decreased by 28.6% (17.0 km) compared with fluid #4. Given the fact that the performance discrepancy of fluid #4 and fluid #1 is prompted by the different water dilutions, it is possible that adding more water to improve cooling properties is an effective way to extend tool life at 200 m/min speed. Fluids #2 and #3 showed similar performance, with the cutting distance decreased by ~16% (20.0 km) compared with fluid #4. The difference between fluid #1 and fluid #3 is the level of the sulfur compound. Therefore, as an extreme pressure (EP) lubricity additive, ~0.3% sulfur content provided good cutting performance (fluid #1), and the increase to 0.8% (fluid #3) of its content resulted in a 14% improvement in cutting distance.

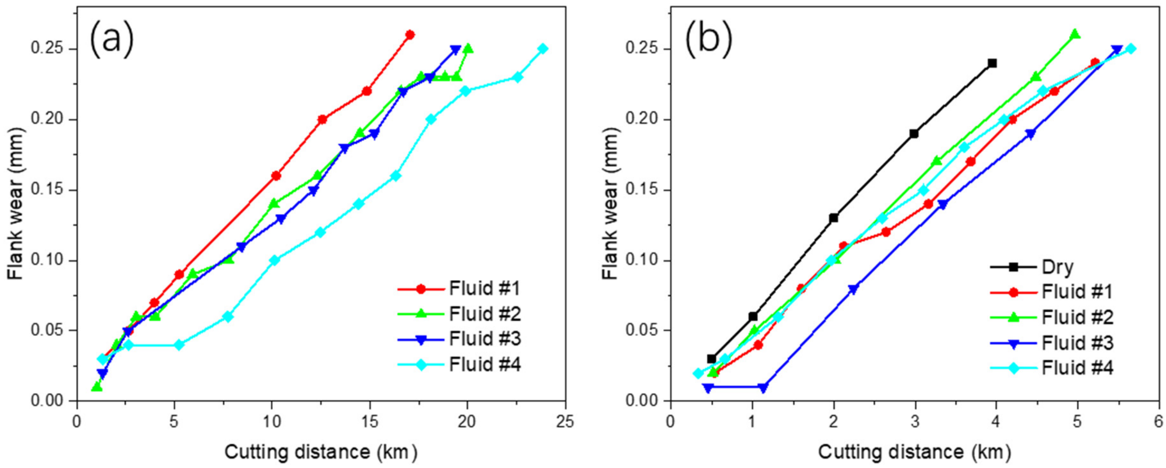

Figure 1. Flank wear vs. cutting distance during turning of CGI with four metalworking fluids at different cutting speeds: (**a**) 200 m/min; (**b**) 300 m/min.

When the cutting speed was increased to 300 m/min, the cutting distance for all the metalworking fluids dropped to less than 6.0 km (Figure 1b). The sharp decrease of the cutting distance at 300 m/min compared with that at 200 m/min was likely due to the dominating factor of higher temperature. As demonstrated by da Silva et al. [10], a higher cutting speed resulted in higher cutting temperature due to increased interaction between the workpiece and the tool. The soluble fluid #4 exhibited the best performance (5.7 km). The full-synthetic fluid #2 showed the least effective performance among all four metalworking fluids, with the cutting distance reaching 4.8 km; nonetheless, it was a 17% increase over the dry condition (4.1 km). Fluids #1 and #3 behaved similarly, with the cutting distances reaching 5.4 km and 5.5 km, respectively. Moreover, there was some delay in the wear of fluid #3 compared to other fluids.

In order to examine the progressive wear on the flank face of the cBN cutting tools, SEM examination was conducted on inserts retrieved at different stages of the cutting process, which was performed at 300 m/min with fluid #4 (Figure 2). An adhered iron-rich region was observed on the cutting edge of the tool (Figure 2d). As the cutting proceeded, the shape of the flank wear scar changed from a long and thin shape (Figure 2a) to a semicircular shape (Figure 2f) with large notch wear at the corners.

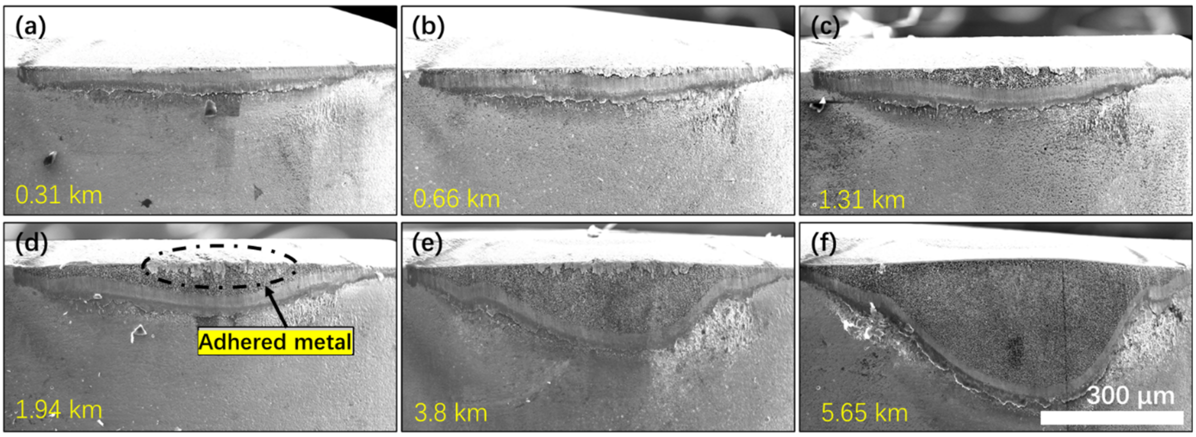

Figure 2. SEM images of the flank face of the inserts at different cutting distances (0.31 km (**a**), 0.66 km (**b**), 1.31 km (**c**), 1.94 km (**d**), 3.8 km (**e**), and 5.65 km (**f**)). Cutting was conducted at 300 m/min with fluid #4.

Figure 3 shows the surface roughness at different locations between the cutting edge (left side) and the inner region of the flank surface (right side). The averaged roughness close to the cutting edge is 213 nm, which gradually reduced to 120 nm at a location close to the coating. This decreasing trend from the cutting edges towards the inner region on the flank surface could be explained by the higher temperature on the cutting edge that may exacerbate the adhesive wear [11–13], resulting in pull-out of the cBN grain and binder, which resulted in higher roughness. On the other hand, in the inner region away from the cutting edge, more abrasive wear was observed, which led to surface flattening. The SEM images of these two different locations are shown in the bottom portion of Figure 3.

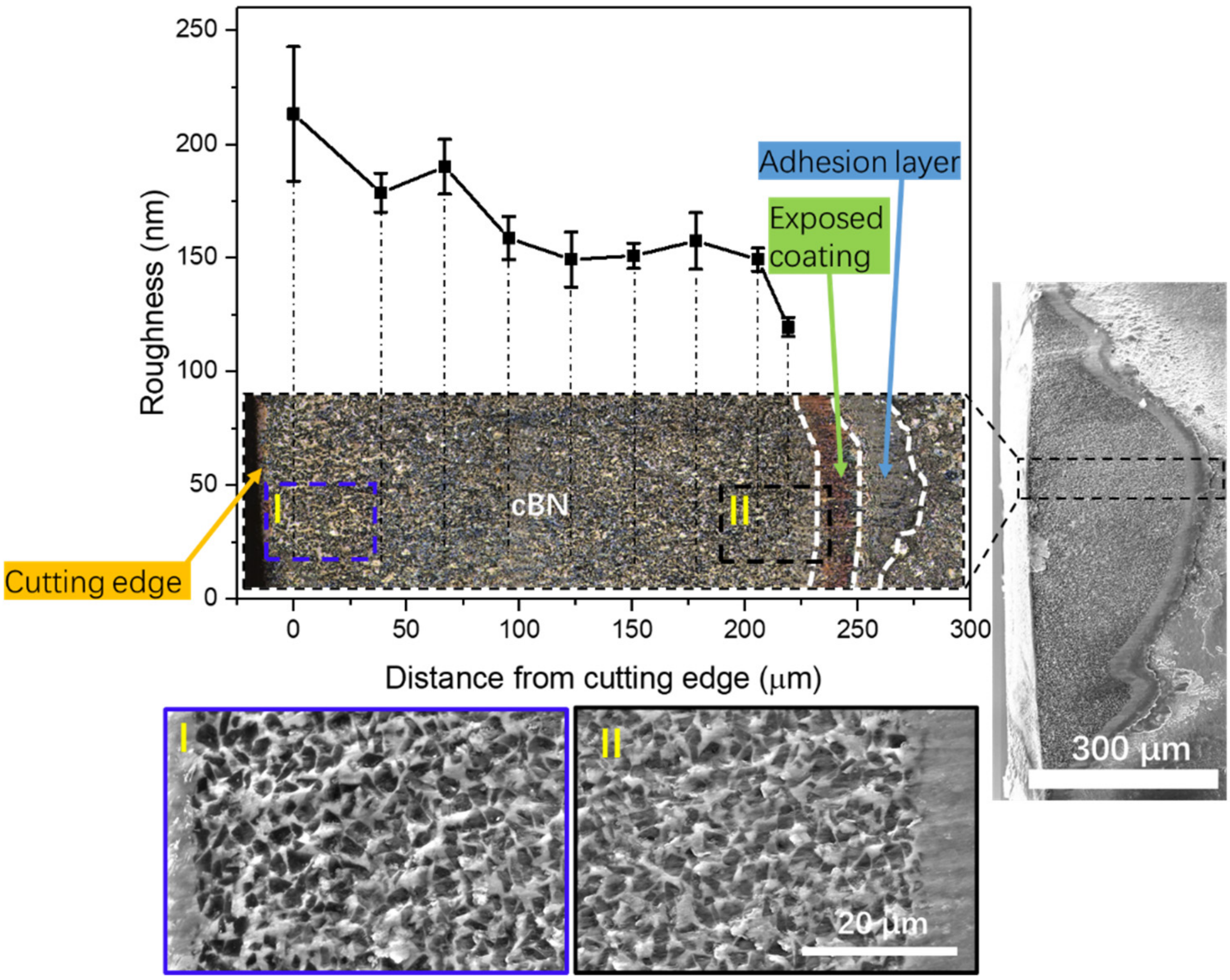

Figure 3. Wear flattening on the flank face of a failed insert using fluid #4. The roughness data is displayed as a function of distance from the cutting edge. The vertical dashed lines match the locations where the roughness data were collected. Bottom: SEM images of the areas close to (**I**) the cutting edge and (**II**) the inner region of the flank surface.

Energy dispersive X-ray spectroscopy (EDX) mappings of O, Fe, and Mg on the worn flank face (Figure 4a) of a failed insert are shown in Figure 4b–d. A higher concentration of Mg and O were observed near the notch wear regions (as illustrated by the white rectangular boxes in Figure 4b,d). This phenomenon was found in all samples tested using all metalworking fluids at 200 m/min cutting speed. Several factors might promote the formation of the notch wear, such as the following: (i) oxidation of the flank surface when it was in contact with air [14,15], (ii) high mechanical stress and thermal gradient in the contact area between the workpiece and the tool [16–18]. These mechanisms may also be associated with the formation and occurrence of MgO in the notch wear region.

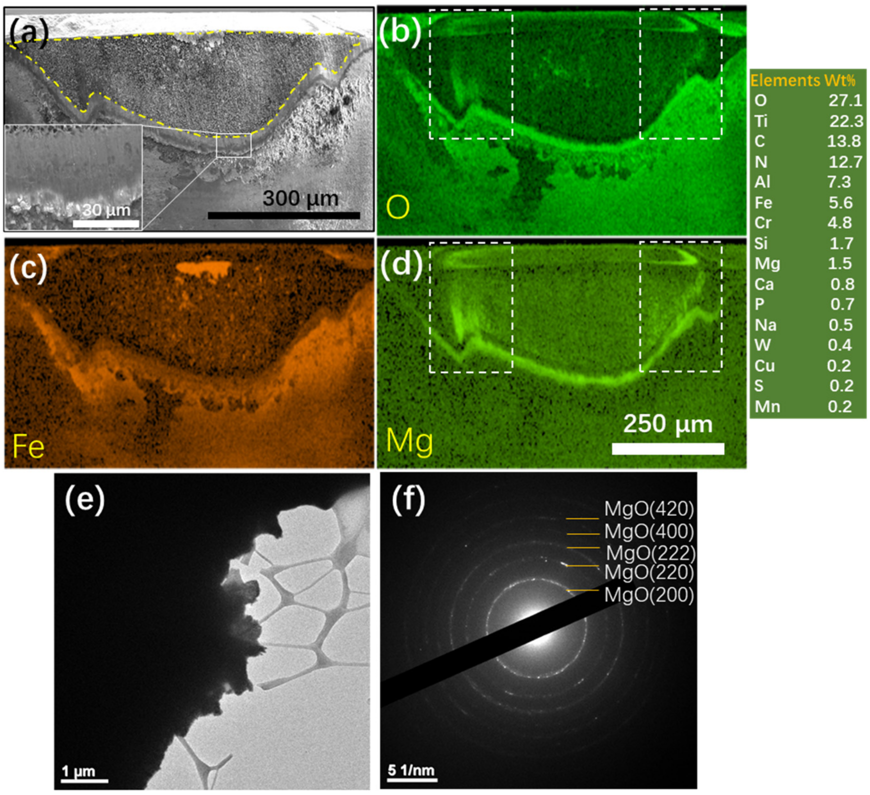

Figure 4. Low-magnification SEM image of the worn flank face of the failed insert (**a**). EDX mapping of O, Fe, and Mg, showing uneven elemental distribution on cBN grain regions cut with fluid #3 at 200 m/min (**b**–**d**). Panels b–d share the same scale bar length. (**e**) TEM image and (**f**) the corresponding selected area electron diffraction (SAED) pattern of scraped deposition on the worn flank face of the insert.

The deposited material on the flank face was collected and examined using TEM (Figure 4e) and selected area electron diffraction (SAED) (Figure 4f). The SAED pattern showed that some collected powder was crystalline, and the diffraction rings were assigned to the (200), (220), (222), (400), and (422) planes of MgO [19]. Both the EDX mapping and TEM/SAED results confirmed our previous hypothesis that Mg reacted to form an oxide. Though with evidence, it is not yet conclusively understood how the MgO phase was formed and its effect on the tool performance, which requires detailed studies in the future.

4. Conclusions

The effects of metalworking fluids on the wear behavior of ceramic coated cBN cutting tools on CGI workpieces were studied in turning operations. Three soluble metalworking fluids and one full-synthetic metalworking fluid were prepared with an additional sulfur compound and different levels of water dilution. Results showed that at 200 m/min cutting speed, the soluble metalworking fluid at 4% dilution and 0.3% sulfur compound exhibited the best performance, with a cutting distance reaching 23.8 km. In contrast, the least effective soluble metalworking fluid at 9% dilution and 0.3% sulfur compound resulted in a 28.6% decrease in the cutting distance (17.0 km) compared to the best one. Increasing the sulfur concentration does not necessarily improve the performance. At a higher cutting speed of 300 m/min, the cutting distance for all four metalworking fluids dropped to shorter than 6.0 km, with the full-synthetic metalworking fluid showing the shortest cutting distance of 4.8 km.

During the turning operation, the ceramic coating on the tool was gradually abraded, and the cBN grains underneath were exposed. Surface roughness on the flank surface decreased from the cutting edges towards the inner region; this could be explained by the higher temperature on the cutting edge, which may exacerbate the adhesive wear. Meanwhile, in the inner region away from the cutting edge, more abrasive wear occurred, leading to flattening. Chemical analysis showed that abundant MgO formed on the worn flank face, especially in the regions near the notch wear. Future studies are highly desired to understand the formation mechanism of the MgO phase and its effect on tool life and performance.

Author Contributions: Conceptualization, R.E., Y.Z. and F.R.; methodology, L.Z., Y.Z., R.E. and F.R.; formal analysis, L.Z. and Y.Z.; investigation, L.Z., R.E., Y.Z. and F.R.; writing—original draft preparation, L.Z.; writing—review and editing, R.E., Y.Z. and F.R.; supervision, Y.Z. and F.R.; project administration, R.E., Y.Z. and F.R.; funding acquisition, R.E., Y.Z. and F.R. All authors have read and agreed to the published version of the manuscript.

Funding: This project was financed in part by a grant from the Commonwealth of Pennsylvania, Department of Community and Economic Development. Any opinions, findings, conclusions, or recommendations expressed herein are those of the author(s) and do not reflect the views of the Commonwealth of Pennsylvania or Carnegie Mellon University.

Institutional Review Board Statement: Not applicable.

Informed Consent Statement: Not applicable.

Data Availability Statement: The data presented in this study are available on request from the corresponding authors.

Acknowledgments: The authors would like to thank Qilin Wei from the Department of Chemistry at Temple University for his technical assistance with TEM characterization. The authors would like to thank Ed Platt and Abigail Meyer from Quaker Houghton for their assistance in machining, and Yixing Zhao and Mark Fennimore from Quaker Houghton for their valuable comments.

Conflicts of Interest: The authors declare no conflict of interest.

References

1. Shao, S.; Dawson, S.; Lampic, M. The mechanical and physical properties of Compacted Graphite Iron. *Mater. Werkst.* **1998**, *29*, 397–411. [CrossRef]
2. Heck, M.; Ortner, H.; Flege, S.; Reuter, U.; Ensinger, W. Analytical investigations concerning the wear behaviour of cutting tools used for the machining of compacted graphite iron and grey cast iron. *Int. J. Refract. Met. Hard Mater.* **2008**, *26*, 197–206. [CrossRef]
3. Dawson, S.; Hollinger, I.; Robbins, M.; Daeth, J.; Reuter, U.; Schulz, H. The Effect of Metallurgical Variables on the Machinability of Compacted Graphite Iron. *SAE Transact.* **2001**, *110*, 334–352. [CrossRef]
4. Evans, R.; Hoogendoorn, F.; Platt, E. Lubrication & Machining of Compacted Graphite Iron. *AFS Trans.* **2001**, 1–8.
5. Gastel, M.; Konetschny, C.; Reuter, U.; Fasel, C.; Schulz, H.; Riedel, R.; Ortner, H.M. Investigation of the wear mechanism of cubic boron nitride tools used for the machining of compacted graphite iron and FGI. *Int. J. Refract. Hard Met.* **2000**, *18*, 287–296. [CrossRef]
6. Monteiro, S.N.; Skury, A.L.D.; de Azevedo, M.G.; Bobrovnitchii, G.S. Cubic boron nitride competing with diamond as a su-perhard engineering material—An overview. *J. Mater. Res. Technol.* **2013**, *2*, 68–74. [CrossRef]
7. Abele, E.; Sahm, A.; Schulz, H. Wear Mechanism when Machining Compacted Graphite Iron. *CIRP Ann.* **2002**, *51*, 53–56. [CrossRef]
8. Tasdelen, B.; Escursell, M.; Grenmyr, G.; Nyborg, L. Machining of gray cast irons and compacted graphite iron. In Proceedings of the Swedish Pro-duction Symposium 2007, Gothenburg, Sweden, 28–30 August 2007; pp. 1–6.
9. Alves, S.M.; Schroeter, R.B.; Bossardi, J.C.D.S.; De Andrade, C.L.F. Influence of EP additive on tool wear in drilling of compacted graphite iron. *J. Braz. Soc. Mech. Sci. Eng.* **2011**, *33*, 197–202. [CrossRef]
10. da Silva, L.R.R.; Filho, A.F.; Costa, E.S.; Pico, D.F.M.; Sales, W.; Guesser, W.L.; Machado, A.R. Cutting Temperatures in End Milling of Compacted Graphite Irons. *Procedia Manuf.* **2018**, *26*, 474–484. [CrossRef]
11. Wang, Z.; Rahman, M.; Wong, Y. Tool wear characteristics of binderless CBN tools used in high-speed milling of titanium alloys. *Wear* **2005**, *258*, 752–758. [CrossRef]
12. Dogra, M.; Sharma, V.S.; Sachdeva, A.; Suri, N.M. Finish Hard Turning of Continuous and Interrupted Surfaces with Cubic Boron Nitride (CBN) and Coated Carbide Tools. *Mater. Manuf. Process.* **2012**, *27*, 523–530. [CrossRef]
13. Gåård, A.; Hallbäck, N.; Krakhmalev, P.; Bergström, J. Temperature effects on adhesive wear in dry sliding contacts. *Wear* **2010**, *268*, 968–975. [CrossRef]

14. Grzesik, W.; Małecka, J. The Oxidation Behaviour and Notch Wear Formation of TiAlN Coated Tools Using Different Oxidation Techniques. *Materials* **2021**, *14*, 1330. [CrossRef] [PubMed]
15. Ozbek, N.A.; Çiçek, A.; Gülesin, M.; Özbek, O. Effect of cutting conditions on wear performance of cryogenically treated tungsten carbide inserts in dry turning of stainless steel. *Tribol. Int.* **2016**, *94*, 223–233. [CrossRef]
16. Kong, J.; Xia, Z.; Xu, D.; He, N. Investigation on notch wear mechanism in finish turning pure iron material with uncoated carbide tools under different cooling/lubrication conditions. *Int. J. Adv. Manuf. Technol.* **2016**, *86*, 97–105. [CrossRef]
17. Ezugwu, E.O.; Wang, Z.M.; Machado, A.R. The machinability of nickel-based alloys: A review. *J. Mater. Process. Technol.* **1999**, *86*, 1–16. [CrossRef]
18. Sharman, A.R.C.; Hughes, J.I.; Ridgway, K. Workpiece surface integrity and tool life issues when turning Inconel 718™ nickel based superalloy. *Mach. Sci. Technol.* **2004**, *8*, 399–414. [CrossRef]
19. Harnchana, V.; Brown, A.P.; Brydson, R.M.; Harrington, J.P.; Hindmarch, A.T.; Marrows, C.H.; Hickey, B.J. TEM characteri-zation of a magnetic tunnel junction. *J. Phys. Conf. Ser.* **2008**, *126*, 012058. [CrossRef]